Geological setting and mineralizing fluids of the Amapari gold deposit, Amapá State, Brazil

Luciana Viana de MELO (1)
Raimundo Netuno VILLAS (2)
José Wilson SOARES (3)
Maria Telma Lins FARACO (4)

Contexte géologique et fluides minéralisants du dépôt aurifère d'Amapari, Etat d'Amapá, Brésil

Géologie de la France, 2003, n° 2-3-4, 243-255, 6 fig., 1 tabl.

Mots clés : Or, Gîte disséminé, Paléoprotérozoïque, Zone de cisaillement, Fluide minéralisateur, Brésil, Amapá.

Key words: Gold ores, Disseminated deposits, Paleoproterozoic, Shear zone, Ore-forming fluids, Orogenic deposits, Brazil, Amapá.

Abstract

The Amapari gold deposit, located in the Guiana Shield of the northeastern Amazon Craton, occurs in a Paleoproterozoic volcano-sedimentary sequence that is correlated with the Vila Nova Metamorphic Suite. This sequence has been metamorphosed under amphibolite conditions, locally deformed by brittle-ductile shear zones and intruded by the ca. *2.0 Ga peraluminous Amapari granite. Primary mineralization has formed two main orebodies - Urucum to the north and Taperebá to the south - with the richest gold contents (up to 30 ppm) contained in the supergene-enriched mantle. The gold is intimately associated with sulfides, chiefly pyrrhotite and subordinate pyrite, chalcopyrite, pentlandite, arsenopyrite, galena and sphalerite.*

Although the overall mineralization is relatively weak, the sulfides are most abundant in the schists. They are less significant in the banded iron formations, and even less in the skarns. Moreover, the more intensely sheared the rocks, the higher the sulfide grades, suggesting a strong structural control for the mineralization. Sulfides + gold occur as disseminations and in thin, discontinuous quartz veins that are generally discordant to the rock foliation. In places, the sulfides are concentrated in laminae parallel to the BIF banding planes.

The mineralizing fluids are characterized as low-salinity (<10 wt.% equiv. NaCl), moderately heated (270 to >420 °C) aqueous-carbonic solutions that may have resulted from devolatilization reactions of deep-seated rocks during the regional metamorphism. These solutions were capable of leaching gold from the rocks with which they interacted and moved along discrete shear zones where gold and sulfides were precipitated in favorable sites in response to T-P-X changes of the fluids. $Au(HS)_2^-$, or a similar complex, seems to have been the most important gold carrier.

Ore mineralogy, structural features, fluid composition, age of the mineralization and geodynamic setting provide supporting evidence to interpret the Amapari deposit as an orogenic gold deposit developed in a continental collision environment.

Resumo

O depósito aurífero Amapari localiza-se no escudo das Guianas, nordeste do cráton Amazônico, no estado do Amapá, Brasil. Ele está hospedado em uma seqüência metavulcanossedimentar, correlacionável com a Suíte Metamórfica Vila Nova, de idade paleoproterozóica, tendo sido metamorfisada em condições da fácies anfibolito, deformada localmente por zonas de cisalhamento em regime dúctil-rúptil e cortada pelo granito Amapari, de caráter peraluminoso, há cerca de 2,0 Ga. A mineralização primária deu origem a dois corpos principais de minério: Urucum, ao norte, e Taperebá, ao sul, porém os teores de ouro mais compensadores (até 30 ppm) são oriundos do manto de enriquecimento supergênico. O ouro está em íntima associação com os sulfetos, principalmente com a

(1) Curso de Pós-graduação em Geologia e Geoquímica, CG-UFPA, Belém (PA), Brazil, lucianavmelo@yahoo.com.br
(2) Departamento de Geologia, CG-UFPA, Belém (PA), Brazil, netuno@ufpa.br
(3) Mineração Itajobi/ Anglo Gold Brasil, soares@anglogold.com.br
(4) Companhia de Pesquisas de Recursos Minerais (CPRM) – Superintendência de Belém, faraco@interconect.com.br

pirrotita e subordinadamente com pirita, calcopirita, pentlandita, arsenopirita, galena e esfalerita.

De um modo geral fraca, a mineralização é mais abundante nos xistos e, em seguida, nas formações ferríferas bandadas e menos ainda nos escarnitos. Além disso, quando mais deformadas as rochas, maiores são os teores dos sulfetos, sugerindo um forte controle estrutural para a mineralização. Sulfetos + Au ocorrem disseminados e em veios de quartzo finos e descontínuos que são, via de regra, discordantes aos planos de foliação das rochas. Ás vezes os sulfetos formam lâminas paralelas aos planos de acamamento das formações ferríferas.

Os fluidos mineralizantes são de baixa salinidade (< equiv. 10% em peso de NaCl), moderadamente quentes (270 a > 420°C) e de composição aquo-carbônica, os quais devem ter resultado de reações de devolatilização em rochas a profundidades relativamente grandes durante o evento metamórfico regional. Essas soluções foram capazes de lixiviar ouro das rochas com as quais elas interagiram, tendo então migrado para as zonas de cisalhamento onde o ouro e os sulfetos foram precipitados em resposta a mudanças nas condições P-T-X dos fluidos. $Au(HS)^-_2$ *ou complexo similar pode ter sido o mais importante agente transportador do ouro.*

O conteúdo mineralógico do minério, as feições estruturais, a composição dos fluidos mineralizantes, a idade da mineralização e o contexto geodinâmico permitem interpretar o depósito Amapari como um depósito orogênico de ouro desenvolvido em ambiente de colisão continental.

Introduction

The discovery of the Serra do Navio manganese ores in the middle 1940s was a major factor that motivated the National Department for Mineral Production (DNPM), the Brazilian Geological Survey (CPRM) and the RADAM Project to carry out regional geological mapping of Amapá State throughout the 1970s. Despite these efforts, difficulties of access, dense forest cover and low investments in the mineral industry have hindered a better knowledge of the State's geology. Ironically, several ore deposits have been discovered in the region and their typological diversity points to multiple mineralizing processes. One of these deposits is the Amapari gold deposit, which is owned by the Itajobi mining company (Anglo Gold Brazil Group). It is located about 18 km east of Serra do Navio town and comprises two orebodies: Urucum and Taperebá.

The purpose of this investigation was to develop a metallogenetic study of the Amapari deposit, with emphasis on the host rocks and wall-rock alteration types, and a characterization of the ore minerals and mineralizing fluids. It aimed also at determining the chemical composition of some minerals in an attempt to infer the protoliths and interpret the conditions under which the deposit rocks were metamorphosed.

Petrographic, mineralogical, chemical and microthermometric data were mostly obtained on drill-core samples from the Urucum orebody. Consequently, our interpretation may not be valid for the entire Amapari deposit.

Regional geology

The Amazon Craton, situated in the northern part of South America and one of the largest cratonic areas of the world, has been tectonically stable since the beginning of the Neoproterozoic (Cordani and Sato, 1999). It is divided into the Guiana Shield (in the north) and the Central Brazil Shield (in the south), the separation being marked by the development of the Paleozoic Amazon Basin. Several models have been proposed to compartmentalize the Amazon region into geotectonic and geochronological domains (Cordani *et al*., 1979; Almeida *et al.*, 1981; Cordani and Brito Neves 1982; Hasui *et al*., 1984; Montalvão and Bezerra 1985; Teixeira *et al*., 1989; Tassinari *et al*., 1996; Tassinari and Macambira 1999; Dall'Agnol *et al*., 2000; Santos *et al.*, 2000). Although conflicting in some aspects, all proposed models accept the existence of an Archean nucleus bordered by shear belts of dominantly Proterozoic age. One of these schemes (Tassinari and Macambira, 1999) defines the Maroni-Itacaiúnas Province (2.2-1.95 Ga), which includes part of Venezuela, Guyana, Suriname, and French Guiana and extends northwest-southeast over Brazil from the still poorly-defined limits with the Central Amazon province to Amapá and Pará states in the east.

The Maroni-Itacaiúnas Province is made up of granite-gneiss complexes with granulitic nuclei that could be reworked portions of the Central Amazon Province (Tassinari, 1997), and volcano-sedimentary sequences that have been deformed and metamorphosed to greenschist- and amphibolite-facies conditions. These sequences have been grouped in the Vila Nova Metamorphic suite. Isotopic data, determined on zircons from felsic granulites (Pb evaporation and U-Pb [SHRIMP]) within the boundaries of the Maroni-Itacaiúnas Province in Amapá State, indicate the presence of a Neo-Archean basement (2.6-3.0 Ga) that was reworked by the Transamazon orogeny 2.1 billion years ago (Lafon *et al.*, 2000). These authors also determined a Pb-Pb age of 2.61-2.56 Ga in zircons from Paleoproterozoic granitoids that occur in the same region, implying inheritance from an Archean crust.

The Amapari deposit area is characterized by a greenstone-like sequence developed in older terrains of the so-called Amapá/NW Pará metallogenetic province or, more specifically, the Serra do Navio/Vila Nova auriferous district (Faraco and Carvalho, 1994).

The regional basement, known as the Guiana Complex (Lima *et al.*, 1974), occurs as nuclei sparsely distributed within Proterozoic terrains. It includes both polymetamorphic rocks, partially reworked during the Transamazon event and represented by granulites, gneisses, amphibolites and migmatites, and associated igneous rocks. U-Pb dating of rocks of the Itamaca Complex (Venezuela), which is correlated with the Guiana Complex, has yielded an age of 3.4 Ga (Montgomery and Hurley, 1978; Montgomery, 1979).

The basement rocks are intruded by the east-west-trending Bacuri Mafic-Ultramafic Complex (BMUC) composed of amphibolites, serpentinites, tremolitites and chromitites. The BMUC rocks are strongly deformed and show a high metamorphic grade (amphibolite facies). Nevertheless, they locally preserve primary structures and textures (Spier, 1999).

The Vila Nova Metamorphic Suite (VNMS) occurs as elongate NW-SE-trending belts whose rocks display subvertical dips, generally to NE. Shear zones are common in response to the brittle to ductile deformation that affected the whole volcano-sedimentary pile. This suite lies unconformably over the Guiana Complex and is characterized as a Proterozoic supracrustal volcano-sedimentary sequence metamorphosed under greenschist- and amphibolite-facies conditions. McReath and Faraco (1997) maintain, based on an Sm-Nd age of 2.264 ± 34 Ma on amphibolites from Ipitinga Ridge (NW Pará State), that the VNMS is chronologically equivalent to the greenstone belts that occur in the north of the Guiana Shield. According to Faraco (1990 and 1997), the VNMS is made up of 1) mafic and ultramafic metavolcanic/metaplutonic rocks, 2) cordierite-anthophyllite-bearing rocks, 3) chlorite-quartz-rich rocks overlying banded iron formations, and 4) continental-derived clastic metasedimentary rocks (quartzites, pelitic schists and metagreywackes).

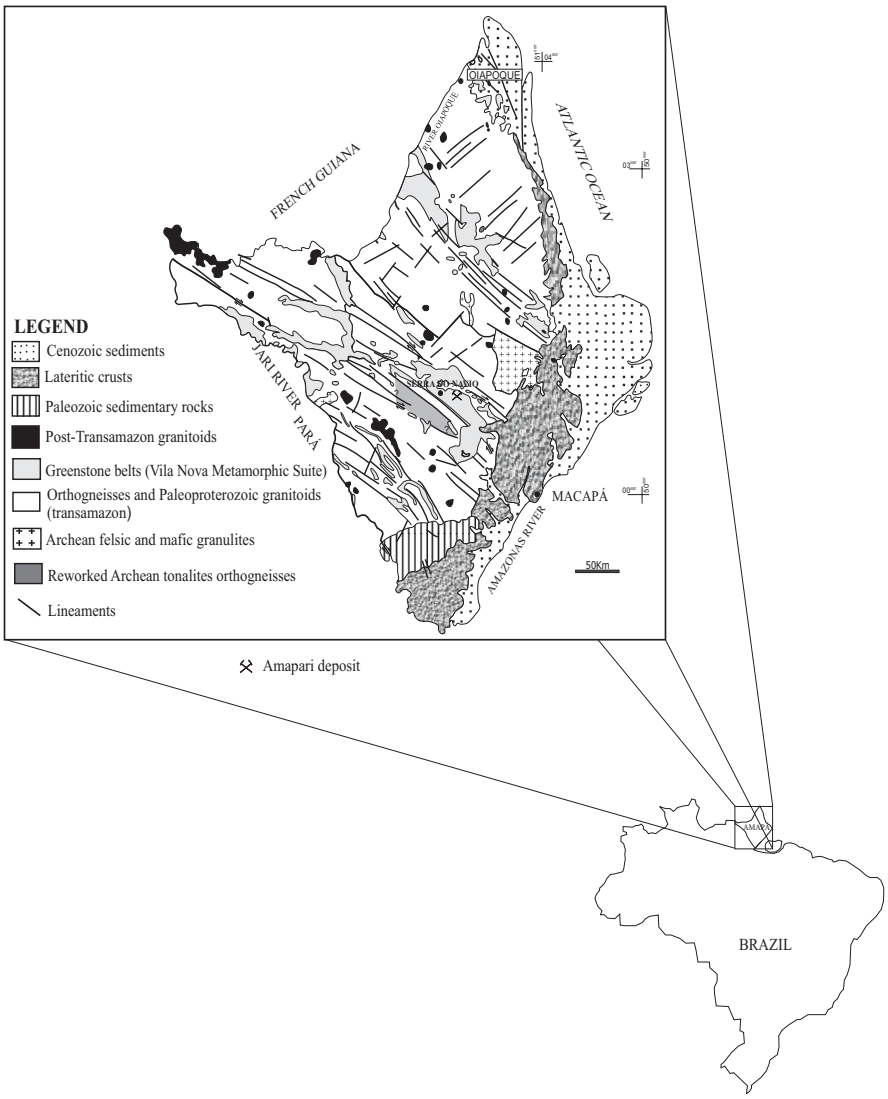

Fig. 1.- Geologic map of Amapá State (modified from Lima *et al.*, 1991).

Fig. 1.- Carte géologique de l'état d'Amapá (selon Lima et al.*, 1991 ; modifiée).*

Rocks of this metavolcano-sedimentary sequence have been thermally metamorphosed and/or hydrothermally altered by the emplacement of several igneous bodies, especially granodiorites, tonalites and syenites. Sulfide-(Au+Ag) mineralization can be observed in hydrothermalized basal metavolcanic rocks. At Ipitinga Ridge, gold occurs associated with volcanogenic sulfides and also in quartz veins hosted by shear zones, or it may be concentrated in rocks affected by supergene processes (Faraco, 1997).

Geology of the Amapari deposit

The Amapari gold deposit (AGD) is hosted by a metavolcano-sedimentary sequence (Fig. 2) of the VNMS that, along with intrusive granitoids, crop out in the vicinity. Pelitic and chemical metasedimentary rocks are far more abundant than the dominantly mafic metavolcanic rocks. The sequence is crosscut by the Amapari granite and affected by discrete brittle to ductile shear zones that deformed and imprinted a conspicuous foliation on the rocks. The granite locally shows a weak foliation developed during the same shear event, and contains small deformed pegmatoid pods that are both concordant and discordant to the foliation planes.

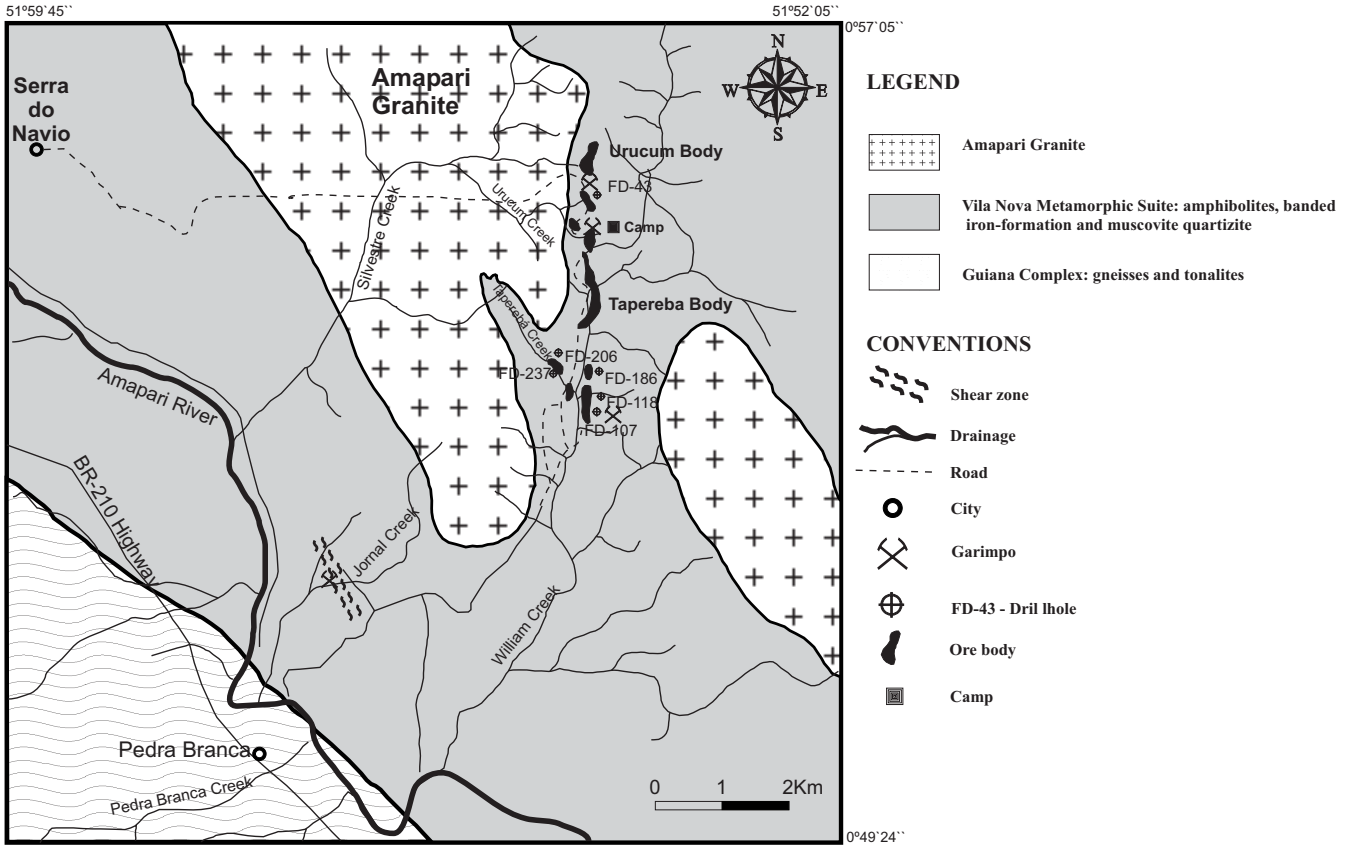

Fig. 2.- Geologic map of the Amapari deposit area (modified from Mineração Itajobi).

Fig. 2.- Carte géologique du gisement d'Amapari (selon Mineração Itajobi, modifiée).

A typical E-W cross-section of the deposit (Fig. 3) displays subvertical contacts between the metasedimentary pile and the Amapari granite. From east to west, the rocks grade from quartz schists to banded iron formations (both oxide and oxide-silicate types) and then to a clastic unit essentially composed of mica schists. These rocks have been weathered and truncated by erosion so that only remnants of an older lateritic crust have been left.

An important characteristic of the metavolcano-sedimentary sequence is the presence of skarns that formed in response to the intrusion of the granitic stock into carbonate rocks associated with the banded iron formations.

The mineralized rocks occur near the contacts of the sequence with the isotropic and hololeucocratic facies of the granite and, in general, show a N-S trend. Two orebodies have already been defined: the Urucum body (to the north) and the Taberebá body (to the south).

Host Rocks and Mineralization

Schists, banded iron formations and skarns are the main rock types that occur in the deposit.

Schists

The schists are dark gray to greenish and present well-developed foliation planes. They are weakly mineralized with sulfides that form disseminations and thin laminae along the foliation planes. Millimeter to centimeter-thick quartz and sulfide veins are discordant to the rock foliation, although a few sulfide veins lie parallel to this structure.

Microscopically, the schists are fine- to medium-grained rocks with a lepidoblastic texture, being composed essentially of biotite, plagioclase, quartz, magnetite and pyrrhotite. Garnet, hornblende, tourmaline and cordierite are the main varietal minerals. The primary accessory assemblage is made up of titanite, apatite and zircon. Some schist varieties present a millimeter-scale compositional banding, whereas others contain pods of clinopyroxene + quartz. The schists have undergone different degrees of ductile deformation. Microfolds, stretched or rotated grains of cordierite, ribbon quartz crystals elongated on foliation planes, and distorted biotite flakes are evidence of deformation by shearing. As a rule, the schists show weak to moderate hydrothermal alteration, having white mica as the most common product.

Based on the mineralogical associations, three schist varieties were identified: a) quartz-plagioclase-biotite schists; b) hornblende-plagioclase-biotite-quartz schists; and c) garnet-cordierite-tourmaline-plagioclase-biotite-quartz schists.

Quartz-plagioclase-biotite schists

Medium grained and strongly foliated with a granoblastic to lepidoblastic texture. Their major constituents average 53% biotite, 29% plagioclase, 11% quartz and 7% pyrrhotite + magnetite. Primary accessory minerals include titanite, apatite and zircon. Hydrothermal alteration is unimportant, but sufficient to generate minor amounts of white mica and opaque phases. Veinlets of quartz + plagioclase transect the rock foliation. A few samples display lens-shaped diopside-rich pods.

Hornblende-plagioclase-biotite-quartz schists

Medium to coarse grained with a granoblastic to nematoblastic texture. The average modal composition is quartz (35%), plagioclase (30%), biotite (25%) and hornblende (10%). The primary accessory assemblage is represented by titanite, opaque phases and zircon. Hydrothermal alteration products are pratically absent, but locally white mica, clinozoisite and carbonates precipitated more intensely.

Garnet-cordierite-tourmaline-plagioclase-biotite-quartz schists

Fine to medium grained, locally coarse grained, with a lepidoblastic to granoblastic texture and a distinctive foliation that in places changes to an irregular compositional banding in which quartz-rich bands are intercalated with bands rich in biotite, tourmaline, plagioclase and opaque phases with minor garnet. The average modal composition is 45% quartz, 26% biotite, 15% opaque phases and 9% plagioclase. Garnet, tourmaline and cordierite occur as varietal minerals and comprise about 5% of the rock volume. Zircon and apatite are the most common accessory phases. These rocks are moderately altered, with white mica and opaque phases being the main hydrothermal products.

Chemical analyses reveal two compositional varieties of biotite distinguished by their FeO and MgO contents: respectively 20.9 and 14.3 wt.% FeO and 9.6 and 12.7 wt.% MgO (Fig. 4A). Their tourmalines have a dravitic composition with $Mg/(Mg+Fe^{2+})$ ratios between 0.53 and 0.77, and CaO^{-} and Na_2O average contents of 0.85% and 1.99 wt.%, respectively (Fig. 4B).

Banded iron formations

Two kinds of BIF (oxide and oxide-silicate types) have been described in the deposit, both presenting a remarkable mineralogical banding. However, where severely disrupted by tectonic processes, the bands may acquire a diffuse character.

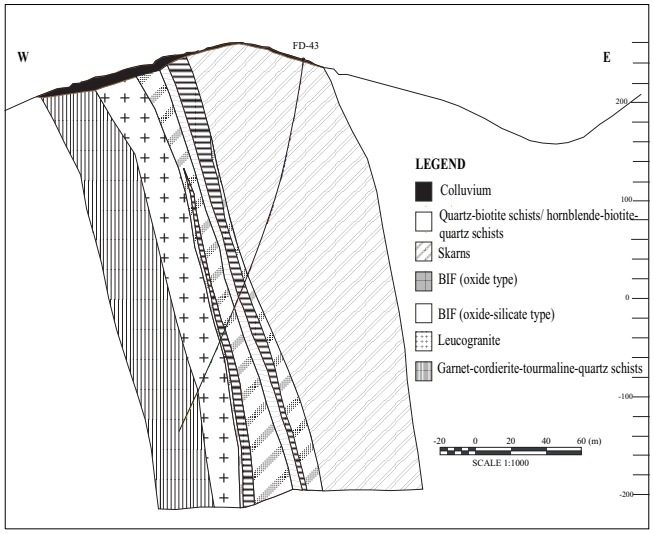

Fig. 3.- W-E cross-section through the Urucum orebody (modified from Mineração Itajobi).

Fig. 3.- Coupe W-E du corps minéralisé Urucum (selon Mineração Itajobi, modifiée).

The oxide-type BIFs present a granoblastic texture and are characterized by intercalations of magnetite-rich and quartz-rich bands. Normally, the bands are uniform with thicknesses varying from a few millimeters to a few centimeters. The dark bands tend to be thicker. On the whole, magnetite and quartz correspond, respectively, to 60 and 40% of the rock volume.

The oxide-silicate-type BIFs show whitish, essentially quartzose, bands intercalated with brownish-green bands enriched in Fe-minerals. Texturally they are granoblastic to nematoblastic and medium-grained. The quartz-rich bands also contain opaque phases, white mica and rare amphibole. Those enriched in Fe-minerals are mostly made up of grunerite and opaque minerals. In the bulk composition, quartz (45-50%) dominates over grunerite (25-40%), whereas the opaque phases, chiefly magnetite, range from 10 to 30%. Veinlets composed of carbonates, white mica or pyrrhotite, transect or are subconcordant to the rock banding.

The chemical composition of the amphibole allows it to be classed as grunerite (Fig. 4C), having $Mg/(Mg+Fe^{+2})$ ratios around 0.3 and Al_2O_3 contents close to 0.25 wt.%.

The schists and BIF are intruded by the hololeucocratic peraluminous Amapari granite, made up dominantly of quartz, albite (average $An^{5.5}$), alkali feldspar, muscovite and minor sillimanite and garnet. Dating of this granite, performed at the Center of Geochronology Research

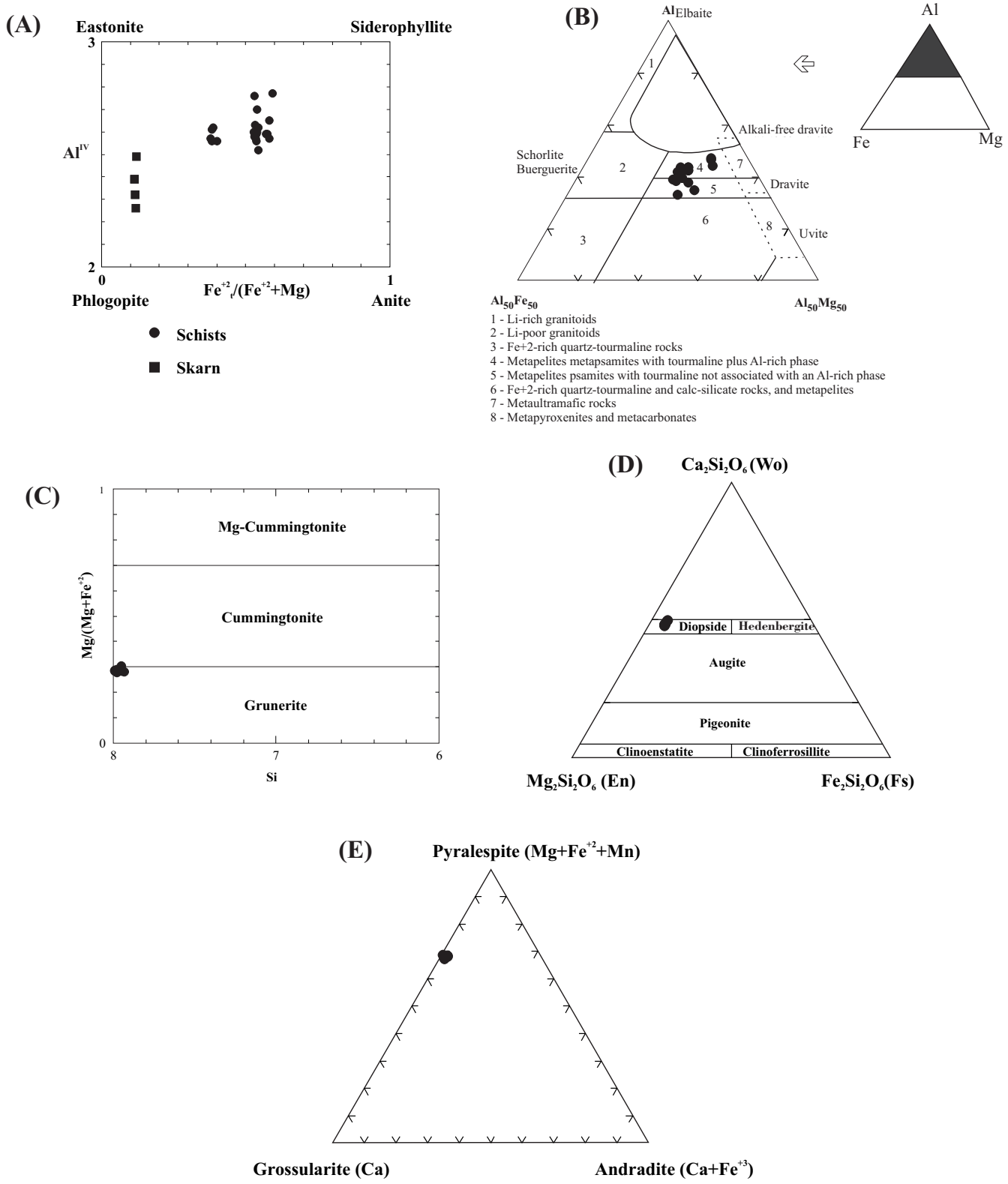

Fig. 4.- Chemical compositional variation of some minerals from the Amapari rocks: **A**) Al^{IV} x $Fe_t^{+2}/(Fe^{+2} + Mg)$ diagram for the micas from schists and skarns; **B**) Al-Fe-Mg diagram for the tourmaline present in the schists. Numbered fields refer to distinct rocks where this mineral is expected to occur; **C**) $Mg/(Mg+Fe^{+2})$ x Si diagram for grunerite from banded iron-formations; **D**) En-Wo-Fs diagram for the skarn pyroxene, allowing it to be classed as diopside; **E**) grossularite-pyralespite-andradite diagram for the skarn garnets.

*Fig. 4.- Variation de la composition chimique de quelques minéraux des roches d'Amapari : **A)** Diagramme Al^{IV} x $Fe_t^{2+}/(Fe^{2+} + Mg)$ pour les micas des schistes et des skarns ; **B)** Diagramme Al-Fe-Mg pour la tourmaline présente dans les schistes. Les champs numérotés se réfèrent aux différentes roches où le minéral doit être présent ; **C)** Diagramme $Mg/(Mg+Fe^{2+})$ x Si pour la grunélite des formations ferrifères rubanées ; **D)** Diagramme En-Wo-Fs pour le pyroxène du skarn montrant qu'il s'agit de diopside ; **E)** Diagramme grossularite-pyralespite-andradite pour les grenats du skarn.*

(CPGeo) of the São Paulo University, yielded a K-Ar age in muscovite of 1826 ± 36 Ma. A more significant value, obtained by the Pb-Pb whole-rock method at the Isotope Geology Laboratory (Pará-Iso) of the Federal University of Pará, was determined at 1993 ± 13 Ma and interpreted as the crystallization age of this intrusion (Jean-Michel Lafon, personal communication).

Although the isotropic facies is dominant, some granitic rocks are fairly well oriented and show kink-bands in plagioclase, strong wave extinction of quartz grains, fracturing of alkali-feldspar phenocrysts and intracrystalline deformation of plagioclase phenocrysts. These features are indicative of a brittle-ductile deformation (Passchier and Trouw, 1996) and suggest that the intrusion may be late tectonic.

Skarns

The skarns resulted from the intrusion of the Amapari granite into carbonate units of the metavolcano-sedimentary sequence. Differing from the schists ands BIFs, the skarns are isotropic and much coarser grained rocks. They generally display two distinct domains: one is diopside-rich and contains garnet porphyroblasts, opaque phases and phlogopite; the other is composed dominantly of carbonate with sparse flakes of phlogopite. Locally the assemblage calcite + periclase is observed. Serpentine, associated with opaque minerals, occurs in the diopside-rich domain filling fractures of the pyroxene grains. Quartz is not common, but occurs either as small pods or along diopside fractures.

Chemically the pyroxene corresponds to a diopside (Fig. 4D) with a homogeneous composition dominated by SiO_2, MgO and CaO (about 96 wt.%) plus minor amounts of FeO and MnO (averages of 2.66% and 0.81%, respectively). Garnet is rich in almandine (36.60-38.51 wt.%), spessartine (25.95-27.40 wt.%) and grossularite (29.31-30.65 wt.%) and poor in pyrope (3.80-4.06 wt.%), andradite (0.81-2.65 wt.%) and uvarovite (<0.16%) (Fig. 4E). The mica present in the skarns has an $Fe_t^{+2}/(Fe^{+2} + Mg)$ ratio around 0.12 and variable Al^{IV} contents (2.32 to 2.49), being characterized as an aluminous phlogopite (Fig. 4A).

Metamorphism and Protoliths of the Host Rocks

The rocks of the Amapari deposit have been subjected to at least two metamorphic events. They were first affected by a regional amphibolite-facies metamorphism that reached minimum temperatures of 530 °C, as inferred from the cordierite-biotite pair present in some schist varieties (Hyndman, 1972; Winkler, 1979). Similar conditions could be deduced in the BIFs from the presence of grunerite, which is indicative of medium-grade metamorphism (French, 1968; Klein, 1973), and also from the dimensions of the quartz grains larger than 0.2 mm (James, 1954; Gross, 1961; Dorr, 1964). In addition, the development of mylonitic textures and stretched garnet porphyroblasts on foliation planes in the schists, as well as rotated cordierite grains and microfolds disturbing these planes, are evidence of a ductile deformational regime under which the rocks were sheared.

The second metamorphic event is related to the intrusion of the Amapari granite. In the contact aureole, where the skarns formed, metamorphic conditions reached the hornblende-hornfels facies. The assemblage calcite + diopside + garnet, common in the Amapari skarns, becomes stable at temperatures near 550 °C and pressures around 2 kbar (Philpotts, 1990). However, temperatures may have exceeded 700 °C, corresponding to the pyroxene hornfels facies, as evidenced by the local occurrence of calcite + periclase (Hyndman, 1972). Except for the formation of small pockets of diopside in some schists, the thermal metamorphism in the schists and BIFs caused no more than local textural changes.

The petrographic data combined with the mineral chemistry enable the schists to be interpreted as rocks derived from pelitic to psammitic sediments having important compositional variations. The association garnet + biotite + cordierite implies derivation from sediments enriched in Mg and Fe, and impoverished in Ca, whereas the local tourmaline concentrations reflect high boron contents. These sediments also contained significant amounts of Ti, expressed as titanite and biotite with average TiO_2 contents of 1.82%. The assemblage hornblende + plagioclase + biotite + quartz and the calc-silicate pockets within the schists may reflect volcanic intercalations (mafic tuffs?) and carbonate impurities, respectively. The BIFs most likely resulted from silica- and iron-rich chemical sediments that gave rise to quartz, magnetite and grunerite, subsequently segregated in distinct bands. The skarns probably derived from Ca- and Mg-rich carbonate rocks, either impure or contaminated by silica-bearing solutions related to the Amapari granite.

Major Structural Features

The two main orebodies lie parallel to the eastern border of the Amapari granite, trending from N-S to NW-SE and dipping 70° either E or W. These directions are broadly coincident with those of the shear zones mapped in the vicinity of the deposit. Field observations show that the granite foliation trends N-S and dips 80 °E, whereas the pegmatoid bodies follow the NE-SW direction. The BIFs are locally sheared along N15°E-trending planes that truncate the N10°W-striking banding surfaces. A 22°NW-dipping lineation marks the direction of movement on the foliation planes.

In drill-hole samples, the BIF banding is crosscut by sulfide-bearing veinlets. Isoclinal microfolds and eye-shaped aggregates obliterate the primary structures. Sulfides in the BIFs are practically restricted to the zones where the bands are more intensely disturbed, and occur as disseminations or along fracture and/or foliation planes. These minerals are also more abundant in the schists that are more strongly deformed, and normally occur in veinlets that are both concordant and discordant to the rock foliation.

The sulfide + Au mineralization

Two kinds of ore can be distinguished in the Amapari gold deposit: 1) primary ore, characterized by sulfide (mostly pyrrhotite) rich zones in which, as a rule, gold and sulfide contents show a positive correlation; and 2) supergene-enriched ore, not discussed in this study, which averages 50 m in thickness and contains the highest gold contents of the deposit (up to 30 ppm).

Epigenetic features represented by veins and veinlets that crosscut the rock foliation are common in the primary ore. Unambiguous syngenetic relationships, on the other hand, are more difficult to pinpoint, the best examples being the sulfide films that lie conformably to the banding planes of the BIFs. Primary disseminated and vein-sulfides have been dated by the Pb-Pb method, yielding an age of 2118±32 Ma (Jean-Michel Lafon, personal communication).

Ore Composition and Modes of Occurrence

Pyrrhotite is the most abundant sulfide, but subordinate amounts of pyrite, chalcopyrite, pentlandite, sphalerite, galena and arsenopyrite are commonly present. The chief gangue minerals are magnetite, quartz, biotite, grunerite, titanite and lesser garnet and diopside.

The sulfides occur as 1) millimeter-thick tabular aggregates, not everywhere continuous, conformable with both the S_o planes of the BIFs and the S_1 planes of the schists, 2) disseminations in the rocks, 3) inclusions in garnet, and 4) veins and veinlets that transect the host rock foliation. Locally the sulfides are concentrated in centimeter-size aggregates. The sulfide abundance decreases from schists to BIFs and then to skarns, and the higher Au contents generally coincide with the most deformed zones, indicating a strong structural control of the mineralization.

Minerography

The data presented here refer only to the Urucum orebody samples.

Pyrrhotite is present as subhedral to anhedral grains in all lithological varieties of the metavolcano-sedimentary sequence. In the schists, it occurs as 1) thin laminae parallel to the foliation planes and in contact with biotite, either in equilibrium or replacing it along cleavage planes, 2) millimeter-size crystals enclosed by titanite aggregates, and 3) vein minerals showing straight to irregular borders against chalcopyrite, pentlandite and quartz. In the BIFs, pyrrhotite displays equilibrium relations with quartz, magnetite and grunerite, whereas in the skarns it forms centimeter-size aggregates, in places included in garnet, or fills fracture planes of diopside and garnet.

Chalcopyrite is everywhere associated with pyrrhotite and is more common in the schists where it occurs as 1) small rounded to subrounded inclusions within 2) fracture minerals in and 3) replacing pyrrhotite grains, and also as anhedral crystals in veins. In rare cases, chalcopyrite is seen associated with pyrrhotite + magnetite, displaying reactive and non-reactive borders with the sulfide and the oxide, respectively. Contacts between chalcopyrite and quartz or biotite are straight. Chalcopyrite is rare in the skarns where it occurs as small clusters together with pyrrhotite or in fractures of diopside and garnet.

Magnetite in the schists is concentrated in an irregular fashion or forms aggregates conformable to the rock foliation. Its crystals commonly have straight contacts with quartz, biotite and pyrrhotite, in places developing triple points at the junction with this sulfide. Unless present in veins or veinlets, it is hardly possible to distinguish between pre-mineralization and ore-stage magnetite in the BIFs. Magnetite is not common in the skarns, where it occupies fracture planes of pyrrhotite aggregates.

Pentlandite is seldom observed and occurs only in the schists as intensely fractured subhedral to anhedral grains. It is everywhere associated with pyrrhotite, and in places coexists in apparent equilibrium with chalcopyrite, biotite and quartz.

Hydrothermal Fluids

A study of fluid inclusions (FI) was carried out on quartz crystals from sulfide-bearing and sulfide-free veins that cut both the schists and the granite. The data show that both aqueous-carbonic and aqueous fluids circulated through the Amapari deposit. Microthermometric results concerning these fluids are summarized in Table 1.

All the aqueous-carbonic FI are primary. At room temperature they display an aqueous phase (F_A) and a carbonic phase (F_C), but some nucleate a vapor carbonic phase (F_{CV}) during the freezing runs. In general, the carbonic phase is dominant, yielding F_C/F_A ratios that vary from 0.5 to 0.95. A few FI show F_A/F_C ratios around 0.6. CO_2-melting temperatures (Tm_{CO2}) are lower than –56.6 °C (Fig. 5A), implying the presence of some contaminants. The carbonic phase homogenizes into the

SYSTEMS	IF TYPES	T_e (°c)	T_{fg} (°c)	Tf_{CO2} (°c)	Tf_{CO2} (°c)	Tht (°C)	Salin	D (g/cm^3)
CO_2-CH_4-H_2O (1)	$L_{(aq)}$ + $CO_{2(L)}$ $L_{(aq)}$ + $CO_{2(l)}$ + $CO_{2(v)}$	-41.5 to -28	-10.0 to -8.0	-59.0 to -56.0	10.0 to 30.0	270 to >420	>10	0.80 to 0.92
NaCl+ $CaCl_2$+H_2O (±$MgCl_2$, ±$FeCl_2$ (1)	L + V	-66.6 to -42.7	-15.5 to -5.8	-	-	150 to 260	9 to 19	1.02 to 1.20
NaCl+$MgCl_2$+$FeCl_2$+ H_2O (2)	L + V, L+V+S	-40.3 to -29	-9.2 to -1.8	-	-	145 to 200	5 to 9	0.86 to 0.98
NaCl+KCl+H_2O (2)	L+V, L+V+S	-24.0 to -19,o	> -5	-	-	170 to 190	3 to 5	0.52 to 0.91
KCl + H_2O (2)	L + V	-16.0 to -10.0	> -5	-	-	200 to 230	2 to 4	0.67 to 0.86
Anomalous fluid (3)	L, L+V, L+V+S	-79.9 to -65.0	-44.5 to -15	-	-	104 to 260	>21	0.91 to 1.09

(1) present in quartz + sulfide veins; (2) present in monomineralic quartz veins; (3) present in both vein type; Te = eutetic temperature ; Tf_g = ice melting tempreature ; Tf_{CO2} = CO_2 melting temperature ; Th_{CO2} = carbonic phase hoimogenization temperature ; Th_t = total homogenization temperature ; Salin = salinity (wt.% equiv. NaCl) ; d = density.

Table 1.- Main characteristics of the hydrothermal fluids related to the Amapari gold deposit.

Tabl. 1.- Caractéristiques principales des fluides hydrothermaux dans le dépôt aurifère d'Amapari.

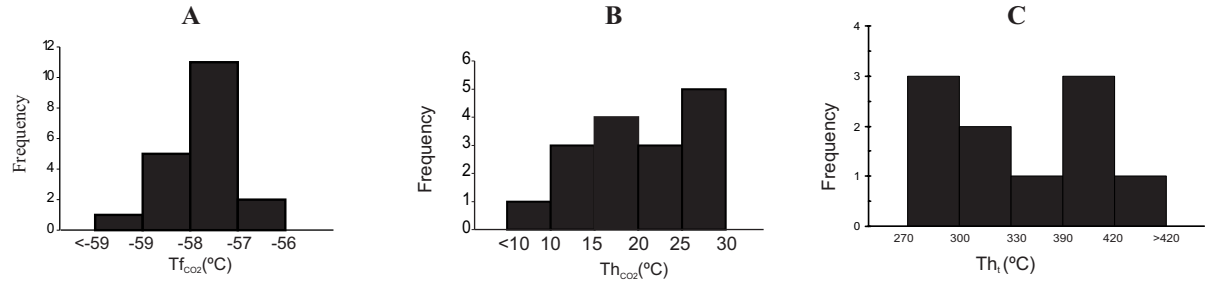

Fig. 5.- Frequency histograms corresponding to the aqueous-carbonic fluid inclusions: **A**) CO_2 melting temperature (Tf_{CO2}); **B**) carbonic phase homogenization temperatures (Th_{CO2}) **C**); total homogenization temperatures (Th_t).

*Fig. 5.- Histogrammes de fréquence correspondant aux inclusions fluides aqueuses carboniques : **A)** Température de fusion de CO_2 (Tf_{CO2}) ; **B)** Températures d'homogénéisation de la phase carbonique (Th_{CO2}) ; **C)** Températures d'homogénéisation totale (Th_t).*

liquid state at temperatures ranging from <10 to 30 °C (Fig. 5B). If CH_4 were the only contaminant, its contents in the carbonic fluid could be estimated at <8% mol. Calculated densities of the carbonic phase for an average of 5% CH_4 yield 0.54 to 0.82 g/cm^3. No clathrate formation is observed, so that salinities were grossly estimated at <10 wt.% equiv. NaCl based on the F_A ice-melting temperatures. Total homogenization temperatures (Th_t) of these FI are in the interval of 270 to >420 °C (Fig. 5C).

Two facts are highly indicative of the aqueous-carbonic fluids being the gold-transporting solutions: 1) the presence of aqueous-carbonic FI only in the sulfide-bearing vein quartz; and 2) the higher the sulfide concentrations the higher the gold contents.

The aqueous fluids show a broad compositional variation, reflecting different sources or different stages of evolution as they migrated and interacted with the deposit rocks. Their salinities are quite variable (3 to >21 wt.% equiv. NaCl) and their Th^t (104 to 260 °C) are lower than those of the aqueous-carbonic fluids (Table 1). The extremely low eutectic temperatures of some of the aqueous fluids (-80 to -65 ºC), due either to the presence of unusual ions in solution (Li+?, Sr^{++}?) or to phenomena of ice metastability (Davis *et al.*, 1990), justify their designation as 'anomalous'.

The different thermal regimes shown by the aqueous-carbonic and the aqueous fluids is suggestive of a distinct evolution. The former are taken to mark the first hydrothermal event, which is related to the development of the shear zones, and were most likely generated by devolatilization reactions of the volcano-sedimentary sequence during the regional metamorphism. The latter may represent magmatic solutions that interacted, to a lesser or greater extent, with the host rocks. Those characterized by NaCl-$CaCl_2$-(±$MgCl_2$-$FeCl_2$)-H_2O solutions and a higher Th^t seem to have had a more intense interaction with the host rocks, from which Ca^{++}, Fe^{++} and Mg^{++} might have been leached. These fluids, together with the 'anomalous' ones, are those with the higher salinities and densities. The aqueous fluids of other compositions and lower Th^t, particularly those rich in KCl, would have had less interaction with the host rock. Finally, the fluids that record the lowest Th^t may represent a mixing of the magmatic fluids with surficial waters during the last stages in the evolution of the Amapari hydrothermal system.

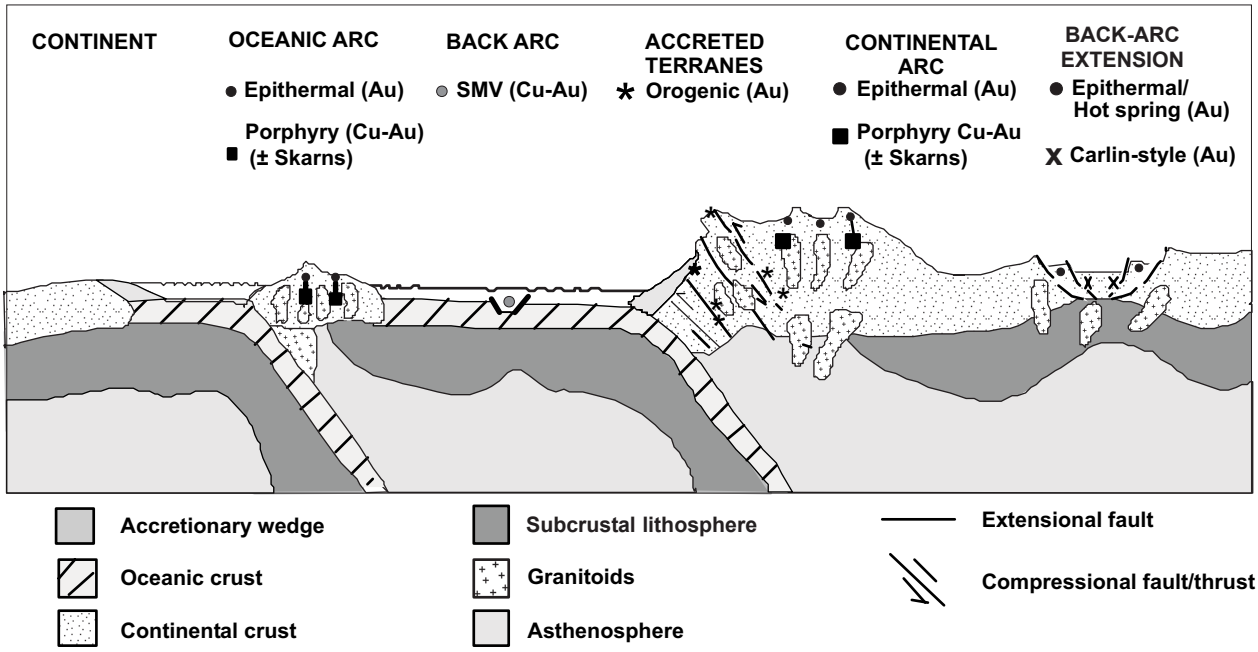

Fig. 6.- Tectonic settings of gold-rich epigenetic mineral deposits, according to Groves *et al*. (1998). The Amapari gold deposit (*) would be set in accretion terrains derived from collisional orogenesis.

Fig. 6.- Contextes tectoniques des gisements aurifères épigénétiques d'après Groves et al. *(1998). Le dépôt aurifère d'Amapari se mettrait en place dans des terrains accrétés, dérivés d'une orogenèse collisionnelle.*

Metallogenetic modeling

The Amapari gold deposit is hosted by a volcano-sedimentary sequence, correlated with the Paleoproterozoic Vila Nova Metamorphic Suite, that underwent regional and thermal metamorphism, in that order. A NW-SE-trending brittle-ductile shear zone was developed during the regional metamorphism, prior to the emplacement of the Amapari granite. This zone may correspond to the secondary splays that resulted from NW-SE regional shearing of the central-south part of Amapá State during the Transamazon thermal-tectonic event. It is quite likely, therefore, that the Amapari deposit was formed in a geodynamic environment similar to that described for French Guiana at the end of the Transamazon event (Vanderhaeghe *et al*., 1998), where crustal thickening and continental collision could have led to partial melting of the crust and the formation of peraluminous granites.

Despite the spatial relations of the orebodies with the Amapari granite, the ages of the mineralization (2118 ± 32 Ma) and of the intrusion (1993 ± 13 Ma) put severe constraints on this igneous body playing any significant role in the deposit genesis. By the same token, and considering the chemical characteristics of the skarn minerals and granite, the possibility of Amapari being a Au-skarn deposit is discarded (Meinert, 1989; 1993).

It is thus suggested that the Amapari deposit belongs to a continental accretion segment, where the common shear zones were highly favorable for the formation of orogenic gold deposits (Groves *et al.*, 1998). The ore mineralogy (dominance of iron sulfides), structural setting (mineralization controlled by shear zones), and mineralizing fluid composition (low-salinity aqueous-carbonic solutions) corroborate this interpretation (Fig. 6). Considering the metamorphic grade and the deformation regime of the rocks, the Amapari gold deposit would have been formed at depths between 7 and 10 km, and hence be classed as a mesozonal deposit (Groves, 1993).

Notwithstanding the many similarities with gold orogenic deposits, important characteristics have not been observed in the Amapari deposit; namely the quartz veins hosted by the shear zones and the remarkable hydrothermal alteration of the host rocks. The mineralizing fluids were apparently poor in silica and not far from equilibrium with the host rocks. It is also possible that the superimposed thermal metamorphism re-equilibrated any hydrothermal products to mineral associations compatible to those produced during the regional metamorphic event. The absence of quartz veins has been also recorded in other shear-zone-hosted lode-gold deposits such as the Lagoa Seca gold deposit, Carajás Mineral Province, southeastern Amazon Craton (Souza, 1999).

As the mineralizing fluids migrated upward along the shear zone, they would have interacted with the rocks and undergone constant compositional and thermal change. The abundance of pyrrhotite indicates a relatively reducing character of the ore fluids and their favorability for transporting gold as a reduced sulfur species. The intimate association between gold and pyrrhotite, the low salinities, and the moderate to high temperatures of the aqueous-carbonic fluids are highly suggestive that gold was carried as a complex such as $Au(HS)_2^-$. Gold precipitation may have resulted from reactions such as $Au(HS)_2^- + FeO \leftrightarrow Au° + FeS + H_2S$ for which FeO was supplied by iron-rich minerals from the host rocks.

Conclusions

This study was mostly based on the Urucum orebody, which represents the northern part of the Amapari gold deposit. A metavolcano-sedimentary sequence, correlated with the Paleoproterozoic Vila Nova Metamorphic Suite, hosts the deposit. Metasedimentary rocks (schists and banded iron formations) are dominant over the essentially mafic metavolcanic rocks and resulted from a regional metamorphic event that reached the amphibolite facies at temperatures above 530 °C. Mylonitic textures, microfolds, stretched garnet crystals and rotated cordierite porphyroblasts observed in the rocks are evidence of a ductile deformational regime related to shear zones.

The Amapari granite, intrusive into that sequence, was responsible for the contact aureole and skarn formation in response to metamorphic-hydrothermal processes on the carbonate units associated with the banded iron formations (BIF). Temperature conditions compatible with the hornblende-hornfels facies reached 500-550 °C, but locally may have been as high as 700 °C, characterizing the pyroxene-hornfels facies. The schists and BIFs were also affected by the thermal metamorphism, although the thermal gradient seems to have been sufficiently high to neither stabilize new mineral associations nor mask regional metamorphic features, so that only local textural changes could be brought about. The Amapari intrusion has been interpreted as a product of granitic magmatism that not only was subsequent to the regional metamorphic peak, but also extended to the late stages of the tectonic event to which the whole deposit area was subjected in Paleoproterozoic times.

Mineralogical and mineral-chemistry data indicate that the schists were derived from pelitic and psammitic sedimentary rocks, some containing expressive amounts of boron and titanium. Volcanic intercalations (mafic tuffs?) or calcium input due to metasomatic processes may account for the presence of hornblende in a few schist varieties. The BIFs comprise both the oxide and the oxide-silicate types that might have been generated from SiO_2- and Fe-rich chemical precipitates. The skarn protoliths were certainly impure carbonate rocks of calcitic to dolomitic composition.

The sulfide + Au mineralization mainly occurs as disseminations. The sulfides are successively more abundant in the skarns, the BIFs and the schists. Regardless of the lithological type, one generally finds that the higher the sulfide content, the higher the gold concentration, although the BIFs present some of the most anomalous Au values. The gold mineralization occurred in a reduced environment, as inferred from the much greater abundance of pyrrhotite among the sulfides.

Available geochronological determinations for the sulfide mineralization (2118±32 Ma) shows it to be younger than the Vila Nova Metamorphic Suite (2264±34 Ma) and older than the Amapari granite (1993±13 Ma). These data indicate that the mineralization was epigenetic and unrelated to the Amapari intrusion. Consequently, the Amapari gold deposit cannot be classed as an Au-skarn deposit, which is corroborated by the chemical composition of some of the skarn minerals.

Fluid-inclusion studies show that both aqueous-carbonic and aqueous solutions circulated throughout the Amapari rocks. The low-salinity (<10 wt.% equiv. NaCl) aqueous-carbonic fluids were most likely the metal-transporting agents under minimum temperatures of 270 to 420 °C. These fluids could have been generated by devolatilization reactions during the regional metamorphic event and focused by shear zones, the gold being carried as a complex such as $Au(HS)_2^-$.

The aqueous fluids are related to the Amapari granite and show varied composition probably due to different degrees of interaction with the rocks through which they percolated. NaCl, KCl, $CaCl_2$, $FeCl_2$ and $MgCl_2$ are the main solutes, the last three largely leached from the country rocks. $NaCl^-$ and/or KCl^-rich solutions were most likely exsolved from the granitic magma. Salinities range from 2 to >21 wt.% equiv. NaCl and minimum trapping temperatures were estimated at 104 to 260 °C, with the lower values credited to mixing with surficial waters.

Despite some dissimilarities, the geodynamic environment, the ore composition, the shear zone-controlled mineralization and the physico-chemical characteristics of the mineralizing fluids constrain the Amapari deposit to the interpreted as an orogenic gold deposit in accordance with the model proposed by Groves *et al.* (1998).

Acknowledgments

We are indebted to the Itajobi Mining Company (Anglo Gold Brazil Group) for permission to visit the deposit area and sample drill-hole cores, in addition to providing

logistic support and making available geological maps and cross-sections. Thanks are due to Dr. Jean-Michel Lafon (UFPA) for the use of unpublished geochronological data and to Dr. Colombo Tassinari (USP) for the K-Ar dating of the Amapari granite. We also acknowledge Drs. Basile Kotschoubey (UFPA) and Roberto Xavier (UNICAMP) for their criticism and insightful comments in a draft version of this paper.

This investigation could not be carried out without the financial support granted by the National Research Council (CNPq) and PRONEX program (Ministery of Science and Technology – MCT). Both are distinctly acknowledged.

References

Almeida F.F.M., HasuyY., Brito Neves B.B., Fuck R.A. (1981) - Brazilian structural provinces: an introduction. *Earth Science Reviews*, **17**, 1-29.

Cordani U.G., Brito Neves B.B. (1982) - The geologic evolution of South America during the Archean and Early Proterozoic. *Revista Brasileira de Geociências*, **12**, 78-88.

Cordani U.G., Sato K. (1999) - Crustal evolution of the South American Platform, based on Nd isotopic systematics on granitoid rocks. *Episodes*, **22** (3), 167-173.

Cordani U.G., Tassinari C.C.G., Teixeira W., Basei M.A.S., Kawashita K. (1979) - Evolução tectônica da Amazônia com base nos dados geocronológicos. *In*: Congresso Geológico Chileno, 2., Arica. Chile, Actas, 137-148.

Dall'Agnol R., Lafon J.-M., Fraga L.M., Scandolara J.E., Barros C.E.M. (2000) - The Precambrian evolution of the Amazonian Craton: one of the last unknown Precambrian terranes in the world. What have we learnt about the structure and evolution of Precambrian shields over the past 10 years? *In*: International Geological Congress, 31. Rio de Janeiro. Abstracts....Rio de Janeiro: CPRM. (CD ROM). K.4.

Davis D.W., Olwenstein T.K., Spencer R. (1990) - Melting behavior of fluid inclusions in laboratory-grown halite crystals in the systems NaCl-H_2O, NaCl-KCl-H_2O, NaCl-$MgCl_2$-H_2O and NaCl-$CaCl_2$-H_2O. *Geochim. Cosmochim Acta* **54**, 591-601.

Dorr J.V.N. (1964) - Supergene iron ores from Minas Gerais, Brazil. *Econ. Geology*, **59**, 1203-1240.

Faraco M.T.L. (1990) - Evolução petrológico-geoquímica das rochas da Suíte Metamórfica Vila Nova na Serra do Ipitinga (NW do Pará). Belém. Universidade Federal do Pará, Centro de Geociências, 346 p. (Dissertação de Mestrado).

Faraco M.T.L. (1997) - Evolução petrológico-geoquímica das rochas e mineralizações associadas à Suíte Vila Nova na Serra do Ipitinga (NW do Pará). Belém. Universidade Federal do Pará, Centro de Geociências, 245 p. (Tese de Doutorado).

Faraco M.T.L., Carvalho J.M. de A. (1994) - A carta metalogenética e previsional do Pará e Amapá. *In*: Congresso Bra Sileiro de Geologia, 38. Camboriú. Anais...SBG. v.1, 291-293.

French B.M. (1968) - Progressive contact metamorphism of the Biwabik Iron-Formation, Mesabi Range Minnesota. *Geol. Surv. Bull*, **45**, 103 p.

Gross G.A. (1961) - Metamorphism of iron-formations and its bearing on their beneficiation. *Canadian Mining and Metall Bulletin*, **54**, 30-37.

Groves D.I. (1993) - The crustal continuum model for late-Archean lode-gold deposits of the Yilgarn Block, Western Australia. *Mineralium Deposita*, **28**, 366-374.

Groves D.I., Goldfarb R.J., Gebre-Mariam M., Hagemann S.G., Robert F. (1998) - Orogenic gold deposits: A proposed classification in the context of their crustal distribution and relationship to other gold deposit types. *Ore Geology Reviews*, **13**, 7-27.

Hasui Y., Haralyi N.L.M., Schobbenhaus C. (1984) - Elementos geofísicos e geológicos da Região Amazônica: Subsídios para o modelo geotectônico. In: Simpósio de Geologia da Amzônia, 2. Manaus. Anais...SGA v.2. 129-147.

Hyndman D.W. (1972) - Petrology of igneous and metamorphic rocks. New York, McGraw-Hill Book Company. 509 p.

James H.L. (1954) - Sedimentary facies of iron-formations. *Econ. Geol.*. **49**, 235-293.

Klein JR. C. (1973) - Changes in mineral assemblages with metamorphic of some banded precambrian iron-formations. *Econ. Geol.*, **68**, 1075-1088.

Lafon J.-M., Avelar V.G., Rossi P., Delor C., Guerrot C., Pidgeon R.T. (2000) - Geochronological evidence for reworked Neoarchean crust during Transamazonian Orogeny (2.1 Ga) in the southeastern Guiana Shield. *In*: International Geological Congress, 31. Rio de Janeiro. Abstracts....Rio de Janeiro: CPRM. (CD ROM).

Lima M.I.C., Montalvão R.M.G., Issler R.S., Oliveira A., Basei M.A.S., Araujo J.F.V., Silva G.G. da. (1974) - Geologia: Folha NA/NB. 22. Macapá. Rio de Janeiro, Projeto RADAM, DNPM. p. 1-120. (Levantamento de Recursos Naturais, 6).

McReath I., Faraco M.T.L. (1997) - Sm-Nd and Rb-Sr systems in part of the Vila Nova metamorphic suite, northern Brazil. *In*: South American Symposium on Isototpe Geology, 1. Campos do Jordão. Extended Abstracts. SAS. p. 194-196.

Meinert L.D. (1989) - Gold skarn deposits – geology and exploration criteria. *In*: Keays R.R., Ramsay W.R.H., Groves D.I. (ed.) The geology of the gold deposits. *Econ. Geol. Monograph* **6**, 537-552.

Meinert L.D. (1993) - Skarns and skarn deposits. *In*: Sheahan P.A. and Cherry M.E. (ed.) Ore deposit models. Geoscience Canada, Reprint Series 6, v. II, 19, 145-162.

Montalvão R.M.G. de, Bezerra P.E.L. (1985) - Evolução geotectônica do Cráton Amazônico durante o Arqueano e o Proterozóico. In: Simpósio de Geologia da Amazônia, 2. Belém. Anais…SBG v.1, 282-297.

Montgomery C.W. (1979) - Uranium-lead geochronology of the Archean Imataca Series, Venezuelan Guyana Shield. *Contributions to Mineralogy and Petrology*, **69**, 167-176.

Montgomery C.W, Hurley P.M. (1978) - Total rock U-Pb and Rb-Sr systematics in the Imataca Series, Guyana Shield, Venezuela. *Earth Planetary Science Letters*, **39**, 281-290.

Passchier C.W., Trouw R.A.J. (1996) - Micro-tectonics. Springer-Verlag. Berlin Heidelberg, 289 p.

Phillips G.N., Groves D.I. (1983) - The nature of Archean gold fluids as deduced from gold deposits of Western Australia. *J. Geol. Soc. Australia*, **30**, 25-39.

Philpotts A.R. (1990) - Principles of igneous and metamorphic petrology. Prentice Hall, New Jersey, 498 p.

Santos J.O.S., Hartmann L.A., Gaudette H.E., Groves D.I., Mcnaughton N.J., Fletcher I.R. (2000) - A new understanding of the provinces of the Amazon Craton based on integration of field mapping and U-Pb and Sm-Nd geochronology. *Gondwana Res.*, **3**, 453-488

Souza C. S. (1999) - Gênese e controle do depósito aurífero de Lagoa Seca, greenstone belt de Andorinhas, Rio Maria – PA. Unpublished MSc. Thesis, Brasilia University, 155 p.

Spier C.A. (1999) - Petrologia e metalogênia dos depósitos de cromita associados ao complexo máfico-ultramáfico Bacuri, AP. Brasília. Universidade de Brasília. Instituto de Geociências. 93 p. (Dissertação de Mestrado).

Tassinari C.C.G. (1997) - The Amazonian Craton. *In*: Wit M. & Aswal. L.D. (eds.) Greenstone Belts. Oxford, Science Publications, Claredon Press. p. 558-566. (Monographs on Geology and Geophysics).

Tassinari C.C.G., Macambira M.J.B. (1999) - Geochronological provinces of the Amazonian Craton. *Episodes*, **22**, 174-182.

Tassinari C.C.G., Cordani U.G., Nutman A.P., Van Schmus W.R., Bittencourt J.S., Taylor P.R. (1996) - Geochronological systematics on basemant rocks from the Rio Negro-Juruena province (Amazon Craton), and tectonic implications. *International Geology Review*, **40**, 71-114.

Teixeira W., Tassinari C.C.G., Cordani U.G., Kawashita K. (1989) - A review of the geochronology of the Amazonian Craton: tectonic implications. *Precambrian Res.*, **42**, 213-227.

Vanderhaeghe O., Ledru P., Thiéblemont D., Egal E., Cocherie A., Tegyey M., Milési J-P. (1998) - Contrasting mechanisms of crustal growth and geodynamic evolution of the Paleoproterozoic granite-greenstone belts of French Guiana. *Precambrian Res.*, **92**, 165-193.

Winkler H.G.F. (1979) - Petrogenesis of metamorphic rocks. 5. ed. New York, Springer – Verlag, 347 p.

Yardley B.W.D. (1994) - Introdução à petrologia metamórfica (Tradução de Reinhardt A. Fuck). Edunb. 340 p.